

Can Divalent Metal Cations Stabilize the Triplex Motif? Theoretical Study of the Interaction of the Hydrated Mg^{2+} Cation with the G–G•C Triplet

Jordi Muñoz,[†] J. L. Gelpí,[‡] Montserrat Soler-López,[§] Juan A. Subirana,[§] Modesto Orozco,^{*,‡,||} and F. Javier Luque^{*,†}

Departament de Fisicoquímica, Facultat de Farmàcia, Universitat de Barcelona, Av. Diagonal s/n, 08028 Barcelona, Spain, Departament de Bioquímica i Biologia Molecular, Facultat de Química, Universitat de Barcelona, Av. Diagonal s/n, 08028 Barcelona, Spain, Departament d'Enginyeria Química, Universitat Politècnica de Catalunya, Av. Diagonal 647, 08028 Barcelona, Spain, and Molecular Modeling and Bioinformatics Unit, Parc Científic de Barcelona, Baldori i Reixach 1-5, 08028 Barcelona, Spain

Received: May 10, 2002; In Final Form: June 17, 2002

A theoretical investigation of the influence of pentahydrated Mg^{2+} cation binding on the Hoogsteen G–G•C triplet motif is presented. Theoretical calculations have been performed by using the structural data of the G–G•C triplet found in the crystallographic structure of the B-DNA duplex d(GCGAATTTCG) [*J. Biol. Chem.* **1999**, 274, 23683–23686]. The investigation involves a variety of theoretical analysis, which includes analysis of geometrical, energetic, electron topology, and electrostatic potential properties. Calculations show the large stabilizing effect of the Mg^{2+} cation on the G–G•C triplet. Such a stabilization mainly arises from the balance of electrostatic interactions between the cation with the three bases in the triplet. However, the cation-induced polarization, which is largely concentrated in the Hoogsteen guanine, also plays a significant contribution to the stabilization of the triplet. The results can be valuable to gain further insight into the cation-induced enhancement of the stability of triple helical structures.

Introduction

Interactions between cations and nucleic acids have been the subject of intense research due to their significance for the structure and function of duplex DNA.¹ Apart from nonspecific accumulation of a diffuse counterion atmosphere around DNA, metal cations can exert their role through a specific coordination to the nucleic acid, including their direct binding to nucleobases,² typically to the N7 atom of guanines.³ The existence of metal–N7 binding has been found not only in DNA but also in different RNAs, including tRNA and ribozymes,^{4,5} where it is suggested to influence both structure and function.

It is also known that monovalent and divalent cations are essential in the stabilization of noncanonical forms of nucleic acids. Both experimental and theoretical data have shown that monovalent ions are crucial to stabilize DNA G-quadruplexes.⁶ Very recently, the X-ray analysis of an RNA (UGGGU)₄ tetraplex has evidenced the existence of a divalent strontium ion placed between every other guanine tetrad plane, mimicking the role of monovalent ions.⁷ Divalent metal cations are also known to influence triple-helical structures,⁸ specially those based on the purine–purine•pyrimidine motif.⁹ Besides electrostatic shielding of phosphate charges, it has been hypothesized that the effect of divalent metal cations is related to its coordination to the N7 atom of the third-strand purines with concomitant polarization on the bases, thus leading in some cases to enhanced hydrogen bonding.^{10,11}

Understanding of the mechanism by which metal cations stabilize the DNA triple helix is limited by the lack of detailed structural data. Vlieghe et al. reported the formation of a G–G•C triplet at the junction between nonamers in the crystallographic structure of the B-DNA duplex d(GCGAATTTCG).¹² The detailed structural features of such a triplet interaction were recently reinvestigated from high-resolution (0.89 Å) crystal X-ray data by Subirana and co-workers.¹³ In the high-resolution structure there are two vicinal G–G•C triplets at the junction between nonamers, each formed between the G10 of one nonamer and the G2•C18 base pair of a neighboring molecule (see Figure 1). The third-strand guanine adopts a Hoogsteen-like orientation in the two triplets. Several Mg^{2+} ions are located in the vicinity of the triplets. In particular, one of them is directly bound to the N7 atom of the G10 in one triplet step. In addition, a chlorine anion is also found around two Mg^{2+} cations, but strikingly it is placed close to the O6 atom of G10 in the vicinal G–G•C triplet. Compared to the reverse Hoogsteen G–G•C motif typical of antiparallel triplexes examined in a previous theoretical study,¹¹ the G–G•C triplet in the X-ray structure reported by Soler-López et al.¹³ adopts a Hoogsteen-like interaction, where the N7-bound cation is proximal to the cytosine (see Figure 1), defining a quite unique triplex recognition pattern.

Structural information on specific ion binding to nucleic acids does not allow a direct insight into the driving forces and energetic contributions that determine ion binding affinity specificity to structural motifs. Such an information can, nevertheless, be gained from ab initio quantum mechanical (QM) approaches. These methods have been previously exploited to describe structural and energetic aspects of the binding of divalent metal cations to nucleic acid bases, base pairs, and nucleotides,¹⁴ and to rationalize specific differences among

* Corresponding authors. E-mail: javier@far1.far.ub.es; modesto@luz.bq.ub.es.

[†] Departament de Fisicoquímica, Universitat de Barcelona.

[‡] Departament de Bioquímica i Biologia Molecular, Universitat de Barcelona.

[§] Universitat Politècnica de Catalunya.

^{||} Parc Científic de Barcelona.

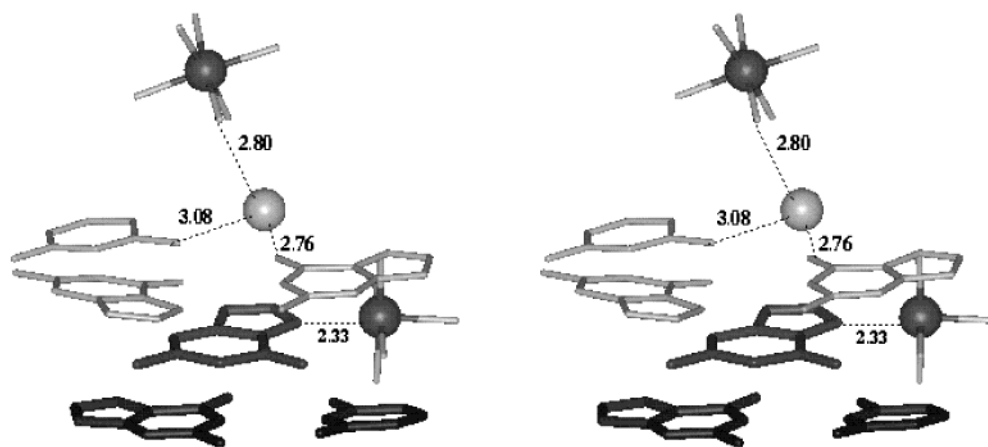


Figure 1. Stereoview of the two G-G-C triplets found in the crystallographic structure of the B-DNA duplex d(GCGAATTCG).¹³ Two hydrated Mg^{2+} cations and one Cl^- anion placed around the triplets are also shown together with selected intermolecular geometrical parameters.

cations in their binding to nucleobases.¹⁵ QM studies further revealed that cation binding to N7 of purine bases has a pronounced influence on the stability of certain base-pairing patterns due to electrostatic and polarization effects whereas other base pairs are mostly unaffected.¹⁶

This study reports a theoretical QM study of the interaction between the Mg^{2+} cation and the Hoogsteen-like G-G-C triplet found in the high-resolution crystallographic structure of the d(GCGAATTCG) duplex.¹² QM calculations are performed to assess the actual strength of different interactions between the nucleic bases and the hydrated cation. In addition to the structural and energetic results, we have investigated the electron density topological properties in hydrogen bonds between bases, as well as the electrostatic properties of the triplet. All this information is used to discuss the role of the Mg^{2+} cation in the stabilization of the G-G-C triplets.

Methods

Systems and Level of Calculation. To understand the role of the Mg^{2+} cation and the neighboring chloride anion, different models were considered: (i) the isolated G-G-C triplet, (ii) the complex of the triplet with pentahydrated Mg^{2+} cation coordinated to the N7 atom of the Hoogsteen-like guanine, (iii) the isolated guanine base, and (iv) the complex between the guanine- $\text{Mg}^{2+}(\text{H}_2\text{O})_5$ and the chloride anion. Simpler models consisting of each separated base alone or interacting with the Mg^{2+} cation or with the Cl^- anion were also examined.

The starting geometry of the different models was taken from the crystallographic data and was subsequently fully optimized at the HF/6-31G(d)¹⁷ level. Interaction energies were computed at the second-order Møller-Plesset¹⁸ perturbation level using the same basis set. The basis set superposition error (BSSE) was corrected using the counterpoise method.¹⁹ The hydrated cation was treated as a single entity in these calculations. The monomer deformation energies were not included, as they are typically more than 1 order of magnitude smaller compared with the intermolecular terms.^{14d,e,15a}

To examine the interaction energy, the complexes were formally divided into four subsystems: the hydrated cation (M) and the three nucleic acid bases (in the following the Watson-Crick and Hoogsteen guanines will be denoted by G_{WC} and G_{H} , respectively). The interaction energy is determined from the difference between the energy of the complex and the energy of the interacting monomers (eq 1). Alternatively, it can be calculated as a sum of six pairwise interaction energies, $E_{\text{int},XY}$ (where X and Y denote M, G_{WC} , G_{H} , C), and the three-body

term, E_3 , as noted in eq 2. Each pairwise interaction energy was determined from the BSSE-corrected difference between the energy of the dimer (XY) and the energy of the monomers (eq 3). Equation 2 allows us to examine the contributions related to the separate interaction between monomers and to the mutual polarization between the interacting subsystems.

$$E_{\text{int}} = E_{\text{GH-GWC-M}}[E_{\text{GH}} + E_{\text{GWC}} + E_{\text{C}} + E_{\text{M}}] \quad (1)$$

$$E_{\text{int}} = E_{\text{int,GHM}} + E_{\text{int,GWCM}} + E_{\text{int,CM}} + E_{\text{int,GHGC}} + E_{\text{int,GWC}} + E_3 \quad (2)$$

$$E_{\text{int},XY} = E_{\text{XY}} - [E_{\text{X}} + E_{\text{Y}}] \quad (3)$$

Topological Properties of Electron Density. The effect of metal binding on the base pairing was examined using two different electron density topological analyses. The first method corresponds to Bader's topological analysis,²⁰ and the second approach relies on the topology of the electron localization function (ELF).^{21,22}

Bader's theory of *atoms in molecules* exploits the charge density gradient field, $\nabla\rho(\mathbf{r})$, to partition the molecular space into basins of attractors, which are usually located at the nuclei. The existence of a bond path linking two nuclei in an equilibrium structure implies that the two atoms are bonded. Such a bond path is characterized by a bond critical point (CP). Because a CP is defined as that point where the electron density gradient field is zero, it can be classified according to its rank (the number of zero eigenvalues of the Hessian matrix) and signature (the algebraic sum of the signs of the eigenvalues). A bond CP is denoted as (3,-1), having one positive and two negative curvatures, which are associated with the charge density along the bond path and the normal directions to the bond path, respectively. Other CPs are associated with local charge density maxima (3,-3), which are located at the nuclei, and to particular geometrical arrangements of bond paths, giving rise to ring (3,+1) and cage (3,+3) CPs depending on whether bond paths are linked as to form a ring or a cage of bonded atoms. Numerous studies have demonstrated that the magnitude of the electron density at the bond CP formed upon hydrogen bonding is strongly correlated with the strength of the hydrogen bond.²³ Accordingly, inspection of the changes in the electron density at the (3,-1) CP can be useful to examine the influence of the cation on the hydrogen-bond interactions between bases.

The topological description of chemical bonds proposed by Silvi and Savin²² relies upon the gradient field analysis of Becke

and Edgecombe's ELF function, $\eta(\mathbf{r})$ (eq 4).²¹ The excess of local kinetic energy is small in regions of space where electrons do not experience the Pauli repulsion, whereas it is large in regions where electrons of the same spin are close to one another. The ELF function permits us to distinguish regions where electrons of the same spin can approach each other from regions where such an approach is difficult, i.e., regions that separate electron pair localization areas from regions where pairs of electron are localized. Therefore, the topological analysis of the gradient of $\eta(r)$ is an alternative procedure to partition the molecular space, where regions are assigned to each local maximum of $\eta(r)$, thus allowing the description of the molecule into core and valence basins. Core basins encompasses nuclei (with $Z > 2$) and valence basins can be classified as mono- (i.e., nonbonded pairs), di-, and polysynaptic (i.e., bonds) depending on the number of core basins with which a common boundary is shared.

$$\eta(\mathbf{r}) = \frac{1}{1 + \left(\frac{D(\mathbf{r})}{D_h(\mathbf{r})} \right)^2} \quad (4)$$

where $D(\mathbf{r})$ and $D_h(\mathbf{r})$ are the excess local kinetic energy due to the Pauli repulsion and the kinetic energy of the homogeneous electron gas of density $\rho(\mathbf{r})$, respectively.

Fuster and Silvi²⁴ have reported a topological scale for the hydrogen-bond strength based on the core-valence bifurcation index (ν). For a given hydrogen bond $\text{A} \cdots \text{H} \cdots \text{B}$, this index is determined from the difference between the lowest value of the ELF function for which all the core basins are separated from the valence ones, $\eta(\mathbf{r}_{\text{cv}})$, and the value of the ELF function at the saddle connection of the valence basins corresponding to the valence disynaptic ($\text{A} \cdots \text{H}$ bond) and monosynaptic (B lone pair) basins, $\eta(\mathbf{r}_{\text{AHB}})$ (eq 5). It has been shown that the increase in ν correlates with a better hydrogen-bond interaction energy.²⁴

$$\nu = \eta(\mathbf{r}_{\text{AHB}}) - \eta(\mathbf{r}_{\text{CV}}) \quad (5)$$

Electrostatic Properties. To gain insight into the effect of the electron density redistribution induced upon cation binding on the interaction between bases, selected electrostatic properties have been examined. Comparison of the molecular electrostatic potential²⁵ computed for each separate base polarized or not by a $2+$ positive charge placed at the location of the Mg^{2+} cation provided qualitative insight into the effect of the cation-induced electron reorganization on the electrostatic interaction between bases. Complementary information was gained from the changes of the dipole moments and electrostatic potential-fitted atomic charges.²⁶

Classical Molecular Interaction Potential (CMIP) Calculations. To investigate the role of Mg^{2+} cations and particularly of the Cl^- anion positioned around the triplet in the X-ray crystallographic structure of the B-DNA duplex d(GCGAAT-TCG),¹⁵ CMIP calculations were performed to determine the interaction energy between the four DNA duplexes in the crystallographic unit cell and either Mg^{2+} or Cl^- ions. The CMIP functional²⁷ expresses the interaction energy between two systems as the addition of the solvent-screened electrostatic energy and a van der Waals term, which is treated by a 6-12 Lennard-Jones expression. The electrostatic energy was computed from a finite-difference solution of the Poisson–Boltzmann equation, where the solvent was treated as a continuum with a dielectric constant of 80, whereas a permittivity of 2 was assigned to the interior of the cavity containing the DNA duplexes. The charge distribution of the DNA duplex was

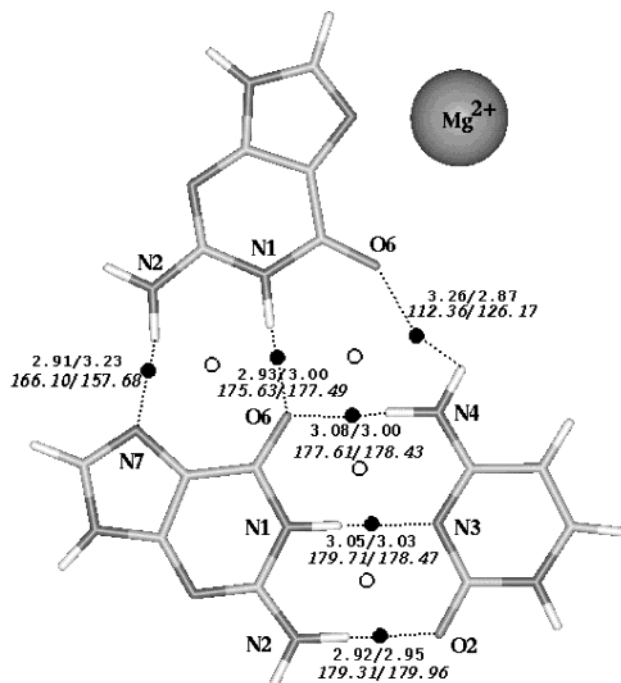


Figure 2. Schematic representation of the G–G•C triplet. Selected geometrical parameters (bond lengths and angles are in Å and degrees) of the intermolecular contacts in the presence (left) or absence (right) of the pentahydrated Mg^{2+} cation. The location of the bond and ring critical points corresponding to the contacts between bases and with the cation is denoted by black and white spheres.

described by using partial atomic charges in the AMBER force-field,²⁸ whereas net charges of $+2$ and -1 were used for Mg^{2+} or Cl^- ions. The dielectric boundary was defined from the atomic van der Waals radii in the AMBER force field, which was also used to assign the atomic hardness parameters for van der Waals calculations. A grid spacing of 0.8 Å was used in all CMIP calculations.

Computational Methods. Ab initio quantum mechanical calculations were performed using the Gaussian98 program.²⁹ Topological analysis was carried out using the PROAIM³⁰ package and the TopMod³¹ program. Electrostatic potential maps were determined using the MOPETE-98³² program. Finally, CMIP calculations were performed using the CMIP computer program.³³

Results

Geometrical Analysis. Figure 2 shows selected geometrical parameters defining the contacts between the different subunits of the G–G•C triplet with and without the pentahydrated Mg^{2+} cation directly bound to the N7 atom of the Hoogsteen-like guanine. In the optimized complex the Mg^{2+} cation is placed at a distance of 2.19 Å from the N7 atom, which agrees with the N7– Mg^{2+} separation of 2.33 Å found in the X-ray crystallographic structure.¹³ Two water molecules link the cation to the guanine O6 atom in the optimized structure, whereas only one water molecule bridges the cation and the O6 atom in the X-ray crystallographic triplet. This difference is likely motivated by the direct coordination of the Mg^{2+} cation to the oxygen of the phosphate group of a vicinal duplex (not directly involved in the formation of the triplet) in the crystallographic structure.

There is satisfactory agreement between the interbase hydrogen-bond distances determined from calculations of the triplet in the presence of the Mg^{2+} cation with the X-ray interatomic values for the cation-bound triplet.³⁴ Thus, the calculated/

experimental³⁴ distances for the contacts between the Hoogsteen guanine (G_H) and either the Watson–Crick guanine (G_{WC}) or cytosine (C) are (G_{WC})N7...(H)N2(G_H) 2.91/2.88 Å, (G_{WC})-O6...(H)N1(G_H) 2.93/2.93 Å, and (C)N4(H)...O6(G_H) 3.26/3.03 Å. For the Watson–Crick pair, the calculated/experimental distances in the presence of the Mg^{2+} cation are (G_{WC})O6...(H)N4(C) 3.08/2.96 Å, (G_{WC})N1(H)...N3(C) 3.05/2.93 Å, and (G_{WC})N2(H)...O2(C) 2.92/2.80 Å. Overall, the difference between predicted and experimental hydrogen-bond distances amounts on average to only 0.10 Å, the largest difference being found in the hydrogen-bond contact between G_H and C (0.23 Å), whereas there is very close agreement in the hydrogen bonds formed between the two guanines (average difference less than 0.02 Å).

According to theoretical calculations for the triplet in the presence and absence of the cation, binding of pentahydrated Mg^{2+} cation strengthens the hydrogen bonding between guanines, as noted in the reduction of the interatomic separation of the (G_{WC})N7...(H)N2(G_H) and (G_{WC})O6...(H)N1(G_H) hydrogen bonds by around 0.3 and 0.1 Å, and weakens the interaction between the Hoogsteen-like guanine and cytosine, as noted in the increase of the (C)N4(H)...O6(G_H) distance by around 0.4 Å. Finally, the hydrogen bonding in the Watson–Crick G·C pair is not very affected upon binding of the cation, as the hydrogen-bond distances are changed, on average, by 0.04 Å.

Comparison of the hydrogen bonds formed in the two triplets in the X-ray crystallographic structure (note that only one triplet is linked to the divalent metal cation, but the other is not) reveals qualitatively similar trends, though the magnitude of the differences in hydrogen-bond distances is sensibly smaller. For instance, the (C)N4(H)...O6(G_H) distance is larger in the cation-bound triplet by around 0.1 Å, whereas theoretical calculations predict an increase of 0.4 Å (see above). The difference between calculated and experimental distances can be likely attributed to the screening influence exerted by the backbone and solvent molecules, as noted in previous theoretical studies.¹⁶

On the basis of the preceding results, it can be concluded that the binding of the Mg^{2+} cation to the N7 atom of the Hoogsteen-like guanine is not expected to lead to apparent geometrical changes in the base pairing in the G–G·C triplet.

Topological Analysis. Selected topological properties of the electron density at the hydrogen bonds between bases in the presence and absence of the pentahydrated Mg^{2+} cation are given in Table 1. The formation of the triplet gives rise to the formation of six bond CPs, which are associated with the bond paths that link the hydrogen-bonded atoms, and four ring CPs, thus satisfying the Poincaré–Hopf relationship.²⁰ The electron density at the bond CP and its laplacian are generally within the range of values typically found for hydrogen-bond contacts, which vary typically in the range 0.002–0.040 and 0.014–0.140 (in atomic units), respectively.^{23,35}

Binding of the cation increases the electron density at the bond CP of the hydrogen bonds between the two guanine bases, particularly at the (G_{WC})N7...(H)N2(G_H) contact. On the contrary, the cation leads to a drastic reduction in the electron density at the (3,–1) CP associated with the Hoogsteen guanine–cytosine pair. In fact, in the presence of the cation the electron density at the CP associated with the Hoogsteen guanine–cytosine pair is so small that it is difficult to label the interaction as a hydrogen bond. Finally, the electron density at the bond CPs of the hydrogen bonds in the Watson–Crick G·C pair remains little affected by the presence of the Mg^{2+} cation. As expected,²³ these changes are in full agreement with the variations in the hydrogen-bond distances (see above).

TABLE 1: Selected Topological Properties^a for the Hydrogen Bonds between Bases in the G–G·C Triplet in the Presence (Plain) or Absence (Italics) of the Mg^{2+} Cation

	ρ	$\nabla^2\rho$	v
Watson–Crick Guanine–Hoogsteen guanine			
N7...(H)N2	0.032	0.098	–0.011
	0.014	0.049	–0.082
O6...(H)N1	0.026	0.090	–0.034
	0.021	0.079	–0.053
Watson–Crick Guanine–Cytosine			
O6...(H)N4	0.019	0.065	–0.069
	0.023	0.078	–0.060
N1(H)...N3	0.025	0.077	–0.031
	0.027	0.080	–0.023
N2(H)...O6	0.027	0.094	–0.047
	0.025	0.087	–0.050
Hoogsteen Guanine–Cytosine			
O6...(H)N4	0.005	0.023	–0.095
	0.015	0.065	–0.072

^a The properties are the electron density (ρ , au) and its laplacian ($\nabla^2\rho$, au) at the bond critical point of the hydrogen bond, and the core-valence bifurcation index (v).

TABLE 2: Total Interaction Energies (E_{int} ; kcal/mol) and Their Pairwise (E_{XY} ; X and Y Denote Hoogsteen and Watson–Crick Guanines, Cytosine, and the Pentahydrated Mg^{2+} Cation) and Three-Body (E_3) Contributions of the Triplet in the Presence or Absence of the Mg^{2+} Cation Determined at the MP2/6-31G(d)//HF/6-31G(d) Level (All Values in kcal/mol)^a

	G–G·C	M...G–G·C ^a	M...G–G ^b
E_{int}	–50.6 (–48.0)	–150.2 (–146.3)	
E_{GHM}		–87.1 (–87.5)	–89.8
E_{GWCM}		–14.2 (–15.7)	–9.5
E_{CM}		+9.7 (+10.6)	
E_{GHGWC}	–14.1 (–13.0)	–14.9 (–12.9)	–19.9
E_{GHC}	–5.5 (–5.3)	–5.1 (–5.2)	
E_{GWCC}	–27.2 (–26.2)	–26.5 (–25.5)	
E_3	–3.8 (–3.6)	–11.7 (–10.2)	–10.4

^a M stands for $Mg^{2+}(H_2O)_5$. HF/6-31G(d) energy values are given in parentheses. ^b Energy contributions for the N7-bound pentahydrated Mg^{2+} cation in the reverse Hoogsteen-like guanine...guanine pair. Values taken from refs 11 and 16b.

The preceding results suggest that the Mg^{2+} mainly affects the hydrogen-bond interactions of the Hoogsteen-like guanine. This hypothesis is reinforced by the cation-induced changes in the index v (see Table 1), which are notably smaller for the Watson–Crick hydrogen bonds than for the Hoogsteen-like ones. Analysis of the cation-induced changes in the index v associated with the two Hoogsteen-like interactions shows that the interaction between guanines is reinforced by the cation, whereas the Hoogsteen guanine–cytosine interaction is weaker in the presence of the cation, in agreement with the changes in the electron density of the corresponding bond CPs (see above). Particularly, the very negative value of the index v for the (C)-N4(H)...O6(G_H) contact, in conjunction with the large interatomic separation (3.26 Å) and the small electron density at the bond CP, suggests that the corresponding hydrogen bonding is largely lost upon binding of the cation. This theory is supported by the fact that whereas in the isolated triplet the bond path links the O6 atom to one of the amino hydrogens of cytosine, in the N7-bound cation complex the bond path connects O6 to the amino nitrogen.

Energetics. Table 2 gives the interaction energies of the triplet with and without the pentahydrated Mg^{2+} cation and their pairwise and three-body contributions computed at the MP2/6-31G(d) and HF/6-31G(d) levels of theory (similar results were

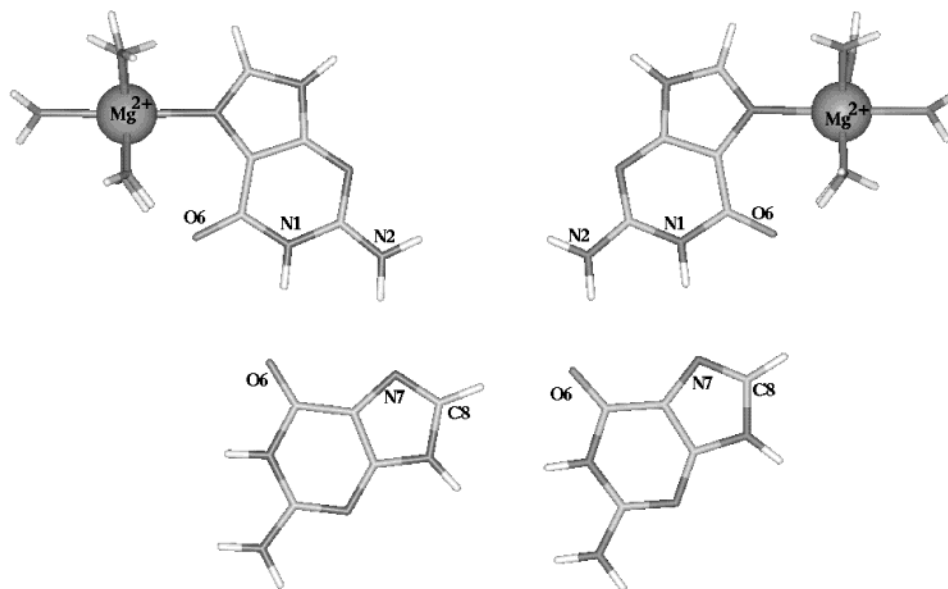


Figure 3. Schematic representation of the pentahydrated Mg^{2+} cation and the two guanine bases in the Hoogsteen (left) and reverse Hoogsteen (right) structures. The arrow denotes the orientation of the dipole moment of the isolated guanine in the complex.

obtained with both methods). The total interaction energy is around 100 kcal/mol larger (in absolute value) in the presence of the Mg^{2+} cation, which mainly stems from the interaction of the cation with the Hoogsteen-like guanine (−87.1 kcal at the MP2/6-31G(d) level). There is also a favorable interaction of the cation with the Watson–Crick guanine (−14.2 kcal/mol), which can be explained by the favorable electrostatic interaction of the cation with the negative electrostatic potential generated by N7 and O6 atoms of the Watson–Crick guanine. In contrast, the interaction of the cation with cytosine is disfavored by +9.7 kcal/mol, as expected from the positive electrostatic potential created by the amino group of cytosine.

The pairwise interaction energies between the bases are generally little affected by the presence of the cation, as noted in the net change of interbase pairwise energies of +0.2 kcal/mol, which is due to a gain of −0.8 kcal/mol in the G•G interaction and a loss of +0.7 and +0.3 kcal/mol in the interactions of Watson–Crick G•C and Hoogsteen G•C pairs (see Table 2). These moderate cation-induced changes in every pair of individual base–base interaction energies are surprising in view of the drastic geometrical and topological changes in the interactions involving the Hoogsteen-like guanine. Clearly, this discrepancy is due to the fact that the interaction energy is due not only to direct hydrogen bonds but also to secondary electrostatic interactions between more distant hydrogen-bond donor and acceptor groups.³⁶ Thus, the stabilization due to shortening of (G_{WC})N7⋯(H)N2(G_{H}) and (G_{WC})O6⋯(H)N1(G_{H}) hydrogen bonds is partly compensated by the unfavorable electrostatic contact between O6 atoms, which are 0.2 Å closer in the presence of the cation. Similarly, the destabilizing effect due to lengthening of the (C)N4(H)⋯O6(G_{H}) hydrogen bond is counterbalanced by the larger separation between the amino groups in the two bases (the N2–N4 distance is increased by around 0.4 Å upon cation binding). As a consequence, caution is necessary when oversimplifications are made, and complex interactions are represented just in terms of a few individual hydrogen bonds.

The difference between the total energy and the sum of pairwise interaction energies must be attributed to the three-body term (eq 2), which is around −8 kcal/mol more favorable in the N7-bound cation complex than in the isolated triplet. Therefore, though the cation-induced stabilization of the triplet

mainly stems from the overall favorable electrostatic interactions with the bases (−91.6 kcal/mol), the 3-body term, related to the polarization of the triad of bases, also contributes remarkably to the stability of the triplet (−11.7 kcal/mol).

For comparison purposes Table 2 also shows the previously published^{11,16b} MP2/6-31G(d)//HF/6-31G(d) energy contributions corresponding to the N7-bound pentahydrated Mg^{2+} cation in the reverse Hoogsteen-like G–G pair (see Figure 3). The interaction energies of the cation with the proximal guanine differ only around 3% in the Hoogsteen or reverse Hoogsteen structures, but the interaction of the cation with the distal (Watson–Crick) guanine is around 50% more stabilizing in the Hoogsteen complex relative to the reverse Hoogsteen structure. The interaction between the two guanines is around 5 kcal/mol larger in the reverse Hoogsteen arrangement. This difference can be explained by the unfavorable electrostatic contribution due to the proximity of the O6 atoms in the Hoogsteen structure, and the formation of a weak hydrogen bond between O6 and (H)C8 atoms in the reverse Hoogsteen complex.^{16b} Finally, the three-body contribution is very similar in the two systems, suggesting that the cation-induced polarization contribution is mainly limited to the effect of the cation on the proximal guanine. Overall, the energies of the N7-bound cation Hoogsteen and reverse Hoogsteen G–G pairs differ by less than 2 kcal/mol. Therefore, it can be stated that the cation-induced stabilization of the G–G•C triplet must be (i) comparable in both Hoogsteen and reverse Hoogsteen arrangements and (ii) sensibly larger than for the A–A•T trio, because the interaction energy of the hydrated Mg^{2+} ⋯G–G complex is around 70 kcal/mol larger than for the hydrated Mg^{2+} ⋯A–A complex.¹¹

Electrostatic Properties. To gain tridimensional insight into the electron redistribution induced upon cation binding, we have compared the electrostatic potential generated by each base computed from the wave function of the isolated base or the wave function polarized by a 2+ point charge placed at the position of the cation in the complex.³⁷

Inspection of Figure 4 shows a marked polarization in the Hoogsteen guanine, leading to a strong enhancement of the negative electrostatic potential around the N7 and O6 atoms and of the positive electrostatic potential around the amino group. The electron shift underlining such a polarization roughly follows the direction of the dipole moment, which increases

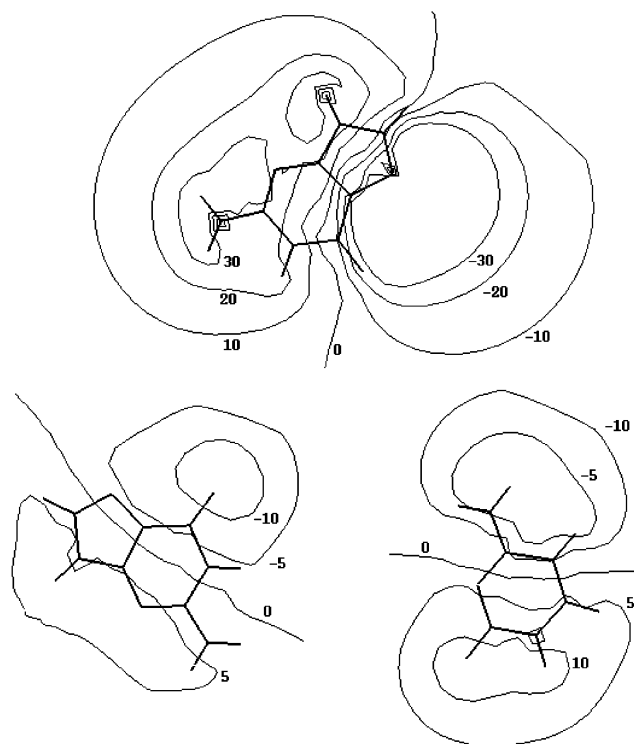


Figure 4. Electrostatic potential difference maps computed at the HF/6-31G(d) level in the molecular plane. These maps were determined by subtracting the electrostatic potential of the isolated base from the electrostatic potential computed from the wave function polarized by a 2+ point charge placed at the location of the Mg^{2+} cation. The values of the isocontour lines are in kcal/mol.

from 8.3 to 15.7 D. The effect of the 2+ point charge on the Watson–Crick bases is notably less important, as noted in the values of the isocontour lines in Figure 4. Accordingly, the magnitude and orientation of the dipoles remain close to the values of the isolated base, with a small increase (1.9 D) for guanine and a small decrease (−1.0 D) for cytosine.

The preceding results suggest that the stabilization of the triplet due to the cation-induced polarization stems mainly from the polarization of the Hoogsteen guanine, leading to a subtle balance of secondary effects. The cation-induced polarization must reinforce the interaction between the two guanines owing to the overlap between the enhanced positive electrostatic regions around the amino and N1(H1) groups in the Hoogsteen guanine and the negative electrostatic potential around N7 and O6 atoms in the Watson–Crick guanine. Nevertheless, such a reinforcement must be limited by the increased repulsion between the enhanced negative electrostatic potential around O6 in the Hoogsteen guanine with O6 in the Watson–Crick guanine.

Role of the Chlorine Anion. A particularly intriguing feature of the G–G•C triplet in the X-ray crystallographic structure of the d(GCGAATTCG) duplex is the presence of a chlorine anion placed close (2.76 Å) to the O6 atom of G10 in the vicinal G–G•C triplet (see Figure 1).¹³ Though it also interacts with the amino N4 atom (3.08 Å) of C2 and with one water molecule that hydrates a proximal Mg^{2+} cation (see Figure 1), such a close contact with O6 cannot be easily understood. One possibility is that the chlorine anion simply occupies an electrostatically favored positioning due to the atmosphere of metal cations at the junction between nonamers. However, because the anion lies at around 3.5 Å along the normal to the five-membered ring of the guanine that interacts with the metal cation (see Figure 1), it might modulate the electron shift



Figure 5. Electrostatic potential difference map computed at the HF/6-31G(d) level for the Hoogsteen guanine. These maps were determined by subtracting the electrostatic potential of the isolated base from (top) the electrostatic potential computed from the wave function polarized by a point charge of −1 placed at the location of the Cl^- anion or from (bottom) the electrostatic potential computed from the wave function polarized by point charges of +2 and −1 placed at the locations of the Mg^{2+} and Cl^- ions. The values of the isocontour lines are in kcal/mol.

redistribution in the Hoogsteen guanine and thus affect the cation-induced stabilization of the triplet.

To investigate the potential role of the chlorine anion in mediating the cation-assisted stabilization of the triplet, the electrostatic potential difference maps of the Hoogsteen guanine computed from the wave function of the isolated base and from the wave functions polarized by (i) a point charge of −1 (placed at the location of the Cl^- anion) or (ii) by point charges of +2 and −1 (placed at the locations of the Mg^{2+} and Cl^- ions, respectively) was recomputed.³⁷ The presence of a −1 point charge in the location of the chlorine anion gives rise to an electron shift from the five-membered ring to the amino N2 group (see Figure 5, top), that is, opposite the electron density redistribution originated upon binding of the cation (see above). Nevertheless, because the magnitude of this effect is small, the electrostatic potential difference map computed in the presence of the two point charges (see Figure 5, bottom) resembles very closely that shown in Figure 4, which argues against a marked influence on the chlorine anion on the cation-induced polarization.

To further investigate the potential influence of the chlorine anion, the partial charges obtained by integration of the electron density over the atomic basins defined by the zero gradient surface were determined for the Hoogsteen guanine interacting with (i) Mg^{2+} cation, (ii) Cl^- anion, and (iii) Mg^{2+} and Cl^- ions simultaneously. The results in Table 5 reveal notable differences in the atomic charges of N7 and N2H₂ groups of the guanine in the presence of the cation or the anion. However, the partial charges of the guanine complexed with the cation

TABLE 3: Partial Charges^a for Isolated Guanine, the Guanine in the Presence of Either Pentahydrated Magnesium Cation or Chlorine Anion, and the Guanine in the Presence of Both Pentahydrated Magnesium Cation and Chloride Anion^b

atom	G	$\text{Mg}^{2+} \cdots \text{G}$	$\text{Cl}^- \cdots \text{G}$	$\text{Mg}^{2+} \cdots \text{G} \cdots \text{Cl}^-$
N1H	-1.275	-1.087 (+0.188)	-1.125 (+0.150)	-1.095 (+0.180)
C2	2.219	2.222 (+0.003)	2.192 (-0.027)	2.222 (+0.003)
N2H ₂	-0.505	-0.447 (+0.058)	-0.557 (-0.052)	-0.486 (+0.019)
N3	-1.637	-1.592 (+0.045)	-1.666 (-0.029)	-1.612 (+0.025)
C4	1.182	1.306 (+0.124)	1.248 (+0.066)	1.327 (+0.145)
C5	0.608	0.528 (-0.080)	0.607 (-0.001)	0.573 (-0.035)
C6	1.753	1.734 (-0.019)	1.724 (-0.029)	1.717 (-0.036)
O6	-1.394	-1.427 (-0.033)	-1.396 (-0.002)	-1.448 (-0.054)
N7	-1.511	-1.673 (-0.162)	-1.432 (+0.079)	-1.666 (-0.155)
C8H	1.506	1.603 (+0.097)	1.509 (+0.003)	1.611 (+0.105)
N9H	-0.946	-1.064 (-0.118)	-1.129 (-0.183)	-1.068 (-0.122)
Mg^{2+}		1.833		1.839
Cl^-			-0.972	-0.950

^a Determined by integrating the electron density in the basin defined by the zero gradient surface at the HF/6-31G(d) level. ^b The differences with regard to the values for the isolated guanine are given in parentheses.

alone or simultaneously with both cation and anion are very similar. These findings, which are in full agreement with the differential polarization effects discussed previously from the electrostatic difference maps, indicate that the influence of the Cl^- anion is surpassed by the effect of the N7-bound Mg^{2+} cation.

The preceding results allow us to rule out a significant role of the chloride anion on the cation-induced stabilization of the triplet and suggest that its location should be determined by the ionic atmosphere in the crystallographic structure. To corroborate this assumption, CMIP calculations were performed for the d(GCGAATTCG) DNA nonamers contained in the crystallographic unit cell. In the absence of the ionic atmosphere, the triplets are surrounded by a large region of negative electrostatic potential (see Figure 6), which justifies the presence of several Mg^{2+} cations around the junction of the nonamers in the crystallographic structure.¹³ However, when the atmosphere of Mg^{2+} cations is considered in the calculations, a small region of favorable interaction energy with a negatively charged point particle appears in the position occupied by the chlorine anion in the crystallographic structure. Accordingly, it can be concluded that the particular structural arrangement of the chlorine anion simply stems from the electrostatic influence position exerted by the atmosphere of metal cations.

Conclusion

The preceding results demonstrate the pronounced effect arising upon binding of metal cations on the energetic and electronic properties of the interacting bases in the Hoogsteen G–G•C triplet. Particularly, the large stabilizing effect of the Mg^{2+} cation on the G–G•C triplet provides a rationale to justify the experimentally known stabilization effect of divalent metal cations on the triple helices. Such a stabilization mainly arises from the balance of electrostatic interactions between the cation with the three bases in the triplet. However, the cation-induced polarization, which is largely concentrated in the Hoogsteen guanine, also provides a significant contribution to the stabilization of the triplet. This finding gives support to the polarization enhancement hypothesis previously suggested by Potaman and Soyfer.¹⁰ The results also allow us to suggest that the net stabilizing effect arising upon N7-binding of the Mg^{2+} cation should be comparable in both Hoogsteen and reverse Hoogsteen G–G•C motifs and clearly larger than that found in A–A•T triplets.¹¹ At this point, we should note that binding of hydrated

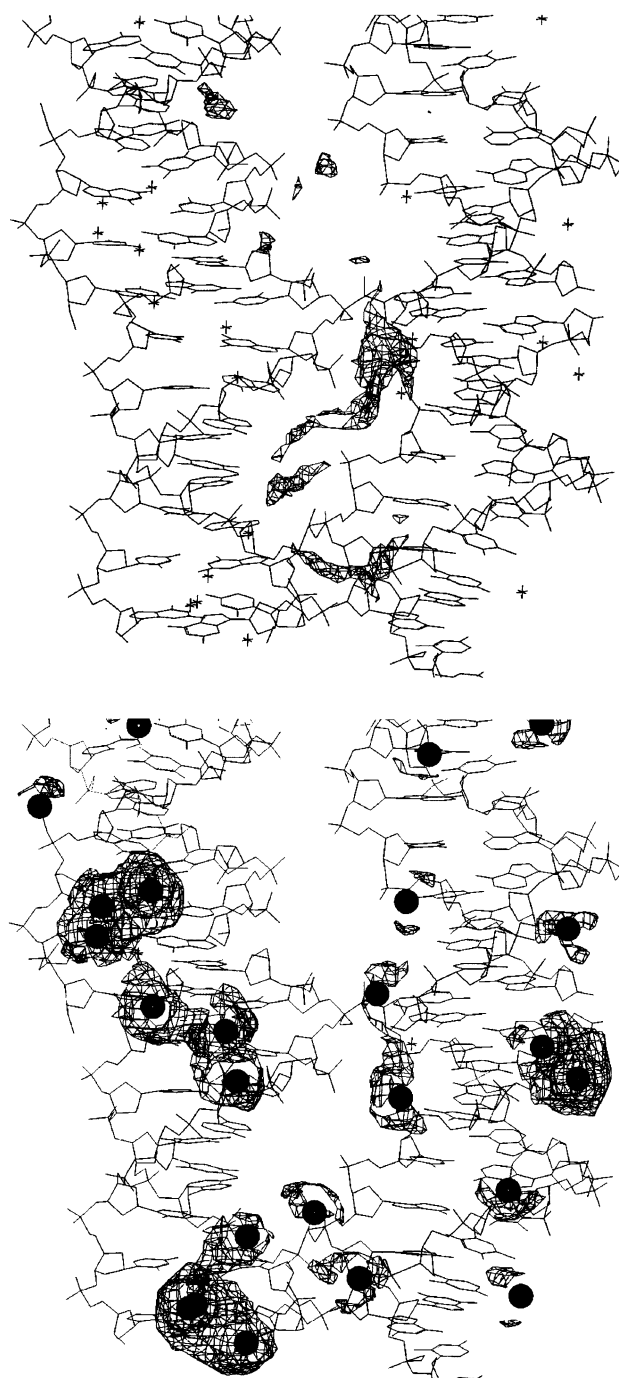


Figure 6. CMIP calculations performed for the DNA nonamers contained in the crystallographic cell unit in absence (top) or presence (bottom) of the cationic atmosphere that surrounds the junction between nonamers. The value of the isocontour surface corresponds to an interaction energy of -14.0 (top) and -4.5 (bottom) kcal/mol. Top: A region of favorable interaction with a Mg^{2+} cation is found around the triplets formed at the junction between nonamers. Bottom: After inclusion of the ionic atmosphere (Mg^{2+} ions denoted by solid spheres), a favorable contact with a Cl^- anion around the two Mg^{2+} proximal to the triplets is clearly seen.

Mg^{2+} cation to the bases in duplex DNA usually takes place with the N7 atom of guanine and only rarely with adenine.^{13,38} Therefore, whether a common mechanism underlies the stabilizing effect of metal divalent cations on the formation of triplexes remains to be elucidated.^{9b,39}

Acknowledgment. We thank Prof. R. F. W. Bader and Prof. B. Silvi for providing their codes for the topological analysis

of the electron density and of the electron localization function. We acknowledge the Centre de Supercomputació de Catalunya for computational facilities. Financial support from the Ministerio de Ciencia y Tecnología (grants PB98-1222 and PM99-0046) is acknowledged. A fellowship from the Departament d'Universitats, Recerca i Societat de la Informació de la Generalitat de Catalunya, to J.M. is kindly acknowledged.

References and Notes

- (1) (a) *Interactions of metal ions with nucleotides, nucleic acids and their constituents*; Sigel, A., Sigel, H., Eds.; Metal Ions in Biological Systems, Vol. 32; Marcel Dekker: New York, 1996. (b) Jerkovic, B.; Bolton, P. H. *Biochemistry* **2001**, *40*, 9406. (c) Nakano, S. I.; Fujimoto, M.; Hara, H.; Sugimoto, N. *Nucl. Acids Res.* **1999**, *27*, 2957.
- (2) (a) Martin, R. B.; Mariam, Y. H. In *Metal Ions in Biological Systems*; Sigel, H., Ed.; Marcel Dekker: New York, 1979; Vol. 8, p 57. (b) Howerton, S. B.; Sines, C. C.; VanDerveer, D.; Williams, L. D. *Biochemistry* **2001**, *40*, 10023.
- (3) (a) Jia, X.; Zon, G.; Marzilli, L. G. *Inorg. Chem.* **1991**, *30*, 228. (b) Froystein, N. A.; Davis, J. T.; Reid, B. R.; Sletten, E. *Acta Chem. Scand.* **1993**, *47*, 649. (c) Marzilli, L. G.; Ano, S. O.; Intini, F. P.; Natile, G. J. *Am. Chem. Soc.* **1999**, *123*, 9133. (d) Duguid, J.; Bloomfield, V. A.; Benevides, J.; Thomas, G. J. *Biophys. J.* **1993**, *65*, 1916. (e) Egli, M.; Williams, L. D.; Fredericks, C. A.; Rich, A. *Biochemistry* **1991**, *30*, 1364. (f) Takahara, P. M.; Frederick, C. A.; Lippard, S. J. *J. Am. Chem. Soc.* **1996**, *118*, 12309. (g) Harper, A.; Brannigan, J. A.; Buck, M.; Hewitt, L.; Lewis, R. J.; Moore, M. H.; Schneider, B. *Acta Crystallogr. D* **1998**, *54*, 1273. (h) Abrescia, N. G. A.; Malinina, L.; Fernandez, L. G.; Huynh-Dinh, T.; Neidle, S.; Subirana, J. A. *Nucl. Acids Res.* **1999**, *27*, 1593. (i) Kankia, B. I. *Nucl. Acid. Res.* **2000**, *28*, 911. (j) Minasov, G.; Tereshko, V.; Egli, M. *J. Mol. Biol.* **1999**, *291*, 83. (k) Robinson, H.; Gao, Y. G.; Sanishvili, R.; Joachimiak, A.; Wang, A. H. J. *Nucl. Acid. Res.* **2000**, *28*, 1760. (l) Kankia, B. I.; Marky, L. A. *J. Phys. Chem. B* **1999**, *103*, 8759. (m) Subirana, J. A.; Abrescia, N. G. A. *Biophys. Chem.* **2000**, *86*, 179. (n) Soler-López, M.; Malinina, L.; Subirana, J. A. *J. Biol. Chem.* **2000**, *275*, 23034.
- (4) (a) Feig, A. L.; Uhlenbeck, O. C. In *The RNA World*, 2nd ed.; Gesteland, R. F., Cech, T. R., Atkins, J. F., Eds.; Cold Spring Harbor Laboratory Press: Cold Spring Harbor, NY, 1999; p 287. (b) Bukhman, Y. V.; Draper, D. E. *J. Mol. Biol.* **1997**, *273*, 1020. (c) Cate, J. H.; Hanna, R. L.; Doudna, J. A. *Nature Struct. Biol.* **1997**, *4*, 553.
- (5) (a) Misra, V. K.; Draper, D. E. *Biopolymers* **1999**, *48*, 113. (b) Tinoco, I.; Kieft, J. S. *Nature Struct. Biol.* **1997**, *4*, 509. (c) Burkhardt, C.; Zacharias, M. *Nucl. Acids Res.* **2001**, *29*, 3910.
- (6) (a) Laughlan, G.; Murchie, A. I. H.; Norman, D. G.; Moore, M. H.; Moody, P. C. E.; Lilley, D. M. J.; Luisi, B. *Science* **1994**, *265*, 520. (b) Hud, N. V.; Smith, F. W.; Anet, F. A. L.; Feigon, J. *Biochemistry* **1996**, *35*, 15383. (c) Phillips, K.; Dauter, Z.; Murchie, A. I. H.; Lilley, D. M.; Luisi, B. *J. Mol. Biol.* **1997**, *273*, 171. (d) Hud, N. V.; Schultze, P.; Feigon, J. *J. Am. Chem. Soc.* **1998**, *120*, 6403. (e) Špačková, N.; Berger, I.; Šponer, J. *J. Am. Chem. Soc.* **2001**, *123*, 3295. (f) Basu, S.; Szwedczak, A. A.; Cocco, M.; Strobel, S. A. *J. Am. Chem. Soc.* **2000**, *122*, 3240.
- (7) Deng, J.; Xiong, Y.; Sundaralingam, M. *Proc. Natl. Acad. Sci. U.S.A.* **2001**, *98*, 13665.
- (8) (a) Hampel, K. J.; Crosson, P.; Lee, J. S. *Biochemistry* **1991**, *30*, 4455. (b) Lyamichev, V. I.; Voloshin, O. N.; Frank-Kamenetskii, M. D.; Soyfer, V. N. *Nucl. Acids Res.* **1991**, *19*, 1633. (c) Xodo, L. E.; Manzini, G.; Quadrioglio, F.; van der Marel, G. A.; van Boom, J. H. *Nucl. Acids Res.* **1991**, *19*, 1633. (d) Bernues, J.; Azorin, F. In *Nucleic Acids and Molecular Biology*; Eckstein, F., Lilley, D. M. J., Eds.; Springer-Verlag: Berlin, 1995; Vol. 9, p 1. (e) Soyfer, V. N.; Potaman, V. N. *Triple-Helical Nucleic Acids*; Springer: New York, 1996; p 100. (f) Sugimoto, N.; Wu, P.; Hara, H.; Kawamoto, Y. *Biochemistry* **2001**, *40*, 9396.
- (9) (a) Sun, J. S.; Helene, C. *Curr. Opin. Struct. Biol.* **1993**, *3*, 345. (b) Bernues, J.; Beltran, R.; Casanovas, J. M.; Azorin, F. *Nucl. Acids Res.* **1990**, *17*, 4067. (c) Collier, D. A.; Wells, R. D. *J. Biol. Chem.* **1990**, *265*, 10652. (d) Malkov, V. A.; Voloshin, O. N.; Soyfer, V. N.; Frank-Kamenetskii, M. D. *Nucl. Acids Res.* **1993**, *21*, 585.
- (10) Potaman, V. N.; Soyfer, V. N. *J. Biomol. Struct. Dyn.* **1994**, *11*, 1035.
- (11) Šponer, J.; Sabat, M.; Burba, J. V.; Doody, A. M.; Leszczynski, J.; Hobza, P. *J. Biomol. Struct. Dyn.* **1998**, *16*, 139.
- (12) Vlieghe, D.; Van Meervelt, L.; Dautant, A.; Gallois, B.; Précigoux, G.; Kennard, O. *Acta Crystallogr., Sect. D* **1996**, *52*, 766.
- (13) (a) Soler-López, M.; Malinina, L.; Liu, J.; Huynh-Dinh, T.; Subirana, J. A. *J. Biol. Chem.* **1999**, *274*, 23683. (b) Soler-López, M.; Malinina, L.; Subirana, J. A. *J. Biol. Chem.* **2000**, *275*, 23034.
- (14) (a) Burda, J. V.; Šponer, J.; Hobza, P. *J. Phys. Chem.* **1996**, *100*, 7250. (b) Šponer, J.; Burda, J. V.; Mejzlík, P.; Leszczynski, J.; Hobza, P. *J. Biomol. Struct. Dyn.* **1997**, *14*, 613. (c) Gadre, S. R.; Pundlik, S. S.; Limaye, C.; Rendell, A. P. *Chem. Commun.* **1998**, 573. (d) Šponer, J.; Sabat, M.; Burda, J. V.; Leszczynski, J.; Hobza, P.; Lippert, B. *J. Biol. Inorg. Chem.* **1999**, *4*, 537. (e) Šponer, J.; Šponer, J. E.; Gorb, L.; Leszczynski, J.; Lippert, B. *J. Phys. Chem. A* **1999**, *103*, 11406. (f) Pelmenchikov, A.; Zilberger, I.; Leszczynski, J.; Famulari, A.; Široni, M.; Raimondi, M. *Chem. Phys. Lett.* **1999**, *314*, 496. (g) Šponer, J.; Šponer, J. E.; Leszczynski, J. *J. Biomol. Struct. Dyn.* **2000**, *17*, 1087. (h) Guerra, C. F.; Bickelhaupt, M.; Snijders, J. G.; Baerends, E. J. *J. Am. Chem. Soc.* **2000**, *122*, 4117. (i) Famulari, A.; Moroni, F.; Široni, M.; Raimondi, M. *Comput. Chem.* **2000**, *24*, 341. (j) Petrov, A. S.; Lamm, G.; Pack, G. R. *J. Phys. Chem. B* **2002**, *106*, 3294. (k) For a review, see: Hobza, P.; Šponer, J. *Chem. Rev.* **1999**, *99*, 3247.
- (15) (a) Burda, J. V.; Šponer, J.; Leszczynski, J.; Hobza, P. *J. Phys. Chem. B* **1997**, *101*, 9670. (b) Šponer, J.; Burda, J. V.; Sabat, M.; Leszczynski, J.; Hobza, P. *J. Phys. Chem. A* **1998**, *102*, 5951. (c) Šponer, J.; Sabat, M.; Burda, J. V.; Leszczynski, J.; Hobza, P. *J. Biomol. Struct. Dyn.* **1998**, *16*, 139. (d) Šponer, J.; Burda, J. V.; Sabat, M.; Leszczynski, J.; Hobza, P. *J. Phys. Chem. B* **1999**, *103*, 2528. (e) Šponer, J.; Burda, J. V.; Leszczynski, J.; Hobza, P. *J. Biomol. Struct. Dyn.* **1999**, *17*, 61. (f) Gresh, N.; Šponer, J. *J. Phys. Chem. B* **1999**, *103*, 11415.
- (16) (a) Šponer, J.; Sabat, M.; Gorb, L.; Leszczynski, J.; Lippert, B.; Hobza, P. *J. Phys. Chem. B* **2000**, *104*, 7535. (b) Muñoz, J.; Šponer, J.; Hobza, P.; Orozco, M.; Luque, F. J. *J. Phys. Chem. B* **2001**, *105*, 6051.
- (17) Hariharan, P. C.; Pople, J. A. *Theor. Chim. Acta* **1978**, *28*, 213.
- (18) Möller, C.; Plesset, M. S. *Phys. Rev.* **1934**, *46*, 618.
- (19) Boys, S. F.; Bernardi, F. *Mol. Phys.* **1970**, *19*, 553.
- (20) (a) Bader, R. F. W. *Atoms in Molecules. A Quantum Theory*; Oxford University Press: Oxford, U.K., 1990. (b) Bader, R. F. W. *Chem. Rev.* **1991**, *91*, 893.
- (21) Becke, A. D.; Edgecombe, K. E. *J. Chem. Phys.* **1990**, *92*, 5397.
- (22) (a) Silvi, B.; Savin, A. *Nature* **1994**, *371*, 683. (b) Savin, A.; Nesper, R.; Wengert, S.; Fässler, T. F. *Angew. Chem., Int. Ed. Engl.* **1992**, *36*, 1809.
- (23) (a) Boyd, R. J.; Choi, S. C. *Chem. Phys. Lett.* **1985**, *120*, 80. (b) Boyd, R. J.; Choi, S. C. *Chem. Phys. Lett.* **1985**, *120*, 80. (c) Bader, R. F. W.; Tang, T. H.; Tal, Y.; Biegler-König, F. W. *J. Am. Chem. Soc.* **1982**, *104*, 4178. (d) Alkorta, I.; Elguero, J. *J. Phys. Chem.* **1996**, *100*, 19367. (e) Mallinson, P. R.; Wozniak, K.; Smith, G. T.; McCormack, K. L. *J. Am. Chem. Soc.* **1997**, *119*, 11502. (f) Roversi, P.; Barzaghi, M.; Merati, F.; Destro, R. *Can. J. Chem.* **1996**, *74*, 4. (g) Mo, O.; Yáñez, M.; Elguero, J. *J. Chem. Phys.* **1992**, *97*, 6628. (h) Alkorta, I.; Rozas, I.; Elguero, J. *Struct. Chem.* **1998**, *9*, 243. (i) Cubero, E.; Orozco, M.; Hobza, P.; Luque, F. J. *J. Phys. Chem. A* **1999**, *103*, 639. (j) Cubero, E.; Orozco, M.; Luque, F. J. *Chem. Phys. Lett.* **1999**, *310*, 445. (k) For review see: Alkorta, I.; Rozas, I.; Elguero, J. *Chem. Soc. Rev.* **1998**, *27*, 163.
- (24) Fuster, F.; Silvi, B. *Theor. Chem. Acc.* **2000**, *104*, 13.
- (25) Scrocco, E.; Tomasi, J. *Top. Curr. Chem.* **1973**, *42*, 95.
- (26) (a) Bonaccorsi, R.; Petrongolo, C.; Scrocco, E.; Tomasi, J. *Theor. Chim. Acta* **1971**, *20*, 331. (b) Momany, F. A. *J. Phys. Chem.* **1978**, *82*, 592. (c) Cox, S. R.; Williams, D. E. *J. Comput. Chem.* **1981**, *2*, 304. (d) Singh, U. C.; Kollman, P. A. *J. Comput. Chem.* **1984**, *5*, 129. (e) Chirlian, L. E.; Frail, M. E. *J. Comput. Chem.* **1987**, *8*, 894. (f) Besler, B. H.; Merz, K. M.; Kollman, P. A. *J. Comput. Chem.* **1990**, *11*, 431. (g) Ferenczy, G. G.; Reynolds, C. A.; Richards, W. G. *J. Comput. Chem.* **1990**, *11*, 159. (h) Breneman, C. M.; Wiberg, K. B. *J. Comput. Chem.* **1990**, *11*, 361. (i) Orozco, M.; Luque, F. J. *J. Comput. Chem.* **1990**, *11*, 909.
- (27) Gelpí, J. L.; Kalko, S. G.; Barril, X.; Cirera, J.; de la Cruz, X.; Luque, F. J.; Orozco, M. *Proteins* **2001**, *45*, 428.
- (28) Case, D. A.; Pearlman, D. A.; Caldwell, J. C.; Cheatham, T. E.; Ross, W. S.; Simmerling, C.; Darden, T.; Merz, K. M.; Stanton, R. V.; Cheng, A.; Vincent, J. J.; Crowley, M.; Ferguson, D. M.; Radmer, R.; Seibel, G. L.; Singh, U. C.; Weiner, P.; Kollman, P. A. *AMBER5*. University of California, San Francisco, 1997.
- (29) Frisch, M. J.; Trucks, G. W.; Schlegel, H. B.; Scuseria, G. E.; Robb, M. A.; Cheeseman, J. R.; Zakrzewski, V. G.; Montgomery, J. A., Jr.; Stratmann, R. E.; Burant, J. C.; Dapprich, S.; Millam, J. M.; Daniels, A. D.; Kudin, K. N.; Strain, M. C.; Farkas, O.; Tomasi, J.; Barone, V.; Cossi, M.; Cammi, R.; Mennucci, B.; Pomelli, C.; Adamo, C.; Clifford, S.; Ochterski, J.; Petersson, G. A.; Ayala, P. Y.; Cui, Q.; Morokuma, K.; Malick, D. K.; Rabuck, A. D.; Raghavachari, K.; Foresman, J. B.; Cioslowski, J.; Ortiz, J. V.; Baboul, A. G.; Stefanov, B. B.; Liu, G.; Liashenko, A.; Piskorz, P.; Komaromi, I.; Gomperts, R.; Martin, R. L.; Fox, D. J.; Keith, T.; Al-Laham, M. A.; Peng, C. Y.; Nanayakkara, A.; Gonzalez, C.; Challacombe, M.; Gill, P. M. W.; Johnson, B.; Chen, W.; Wong, M. W.; Andres, J. L.; Gonzalez, C.; Head-Gordon, M.; Replogle, E. S.; Pople, J. A. *Gaussian 98*, revision A.7; Gaussian, Inc.: Pittsburgh, PA, 1998.
- (30) Biegler-König, F.; Bader, R. F. W.; Tang, T. H. *J. Comput. Chem.* **1982**, *3*, 317.
- (31) Noury, S.; Krokidis, X.; Fuster, F.; Silvi, B. TopMod package. University Pierre et Marie Curie, 1997.
- (32) Luque, F. J.; Alhambra, C.; Orozco, M. MOPETE program. University of Barcelona, 1998.
- (33) Gelpí, J. L.; Luque, F. J.; Orozco, M. CMIP program. University of Barcelona, 2000.

(34) The experimental values correspond to the hydrogen-bond distances determined for the G–G•C triplet linked to the Mg^{2+} cation in the X-ray crystallographic structure.

(35) (a) Koch, U.; Popelier, P. L. A. *J. Phys. Chem.* **1995**, 99, 9747. (b) Popelier, P. L. A. *J. Phys. Chem. A* **1998**, 102, 1873. (c) Hobza, P.; Šponer, J.; Cubero, E.; Orozco, M.; Luque, F. J. *J. Phys. Chem. B* **2000**, 104, 6286.

(36) (a) Jorgensen, W. L.; Severance, D. L. *J. Am. Chem. Soc.* **1991**, 113, 209. (b) Pranata, J.; Wjersche, S. G.; Jorgensen, W. L. *J. Am. Chem. Soc.* **1991**, 113, 2810. (c) Šponer, J.; Leszczynski, J.; Hobza, P. *J. Phys.*

Chem. **1996**, 100, 1965. (d) Uchimaru, T.; Korchovec, J.; Tsuzuki, S.; Matsumara, K.; Kawahara, S. *Chem. Phys. Lett.* **2000**, 318, 203.

(37) Values determined at the HF/6-31G(d) level using the geometries of the monomers in the complex with the metal cation.

(38) Chiu, T. K.; Dickerson, R. E. *J. Mol. Biol.* **2000**, 301, 915.

(39) Khomyakova, E. B.; Gousset, H.; Liquier, J.; Huynh-Dinh, T.; Gouyette, C.; Takahashi, M.; Florentiev, V. L.; Taillandier, E. *Nucl. Acids Res.* **2000**, 18, 3511.